Many-body approach to Luttinger's theorem for the Kondo lattice

Steffen Sykora[1] and Klaus W. Becker[2]
[1]*Leibniz-Institute for Solid State and Materials Research, IFW-Dresden, 01069 Dresden, Germany*
[2]*Institut für Theoretische Physik, Technische Universität Dresden, D-01062 Dresden, Germany*

(Received 27 August 2018; revised manuscript received 22 November 2018; published 26 December 2018)

A numerical verification of Luttinger's theorem, based on a recently developed many-body approach, is given for the Kondo-lattice model. For a two-dimensional lattice the completely localized spins ($S = 1/2$) are found to contribute to the Fermi sea volume as if they were electrons, which is in agreement with Oshikawa's topological proof of Luttinger's theorem. Underpinning this result we explicitly calculate the momentum-resolved one-particle spectral function showing nearly dispersionless excitations clearly below the Fermi level for different values of the conduction electron filling. Numerical integration over momentum and energy always leads to the correct particle number of the localized spins according to the well-accepted picture of a large Fermi surface. In this paper, a first many-body approach is shown, which is able to reproduce the correct value of Luttinger's theorem for this model.

DOI: 10.1103/PhysRevB.98.245139

I. INTRODUCTION

The minimal model of heavy-fermion systems is the Kondo-lattice model. It is formed by a periodic array of localized spins which are coupled to a system of free conduction electrons. A theoretical description of the Kondo-lattice physics is demanding since perturbation theory in the Kondo coupling j_K is essentially singular at $j_K = 0$ (see, for example, Ref. [1]). Therefore, effects up to infinite order in j_K have to be systematically included in a study of this model. One possible way to circumvent this difficulty is to apply a so-called large-N expansion, which is based on the idea that due to the large spin-orbit coupling in heavy-fermion compounds [2] the number of spin components of the electrons can be extended to a very large number N. In particular, the limit $N \to \infty$ enables the negligence of the Ruderman-Kittel-Kasuya-Yosida (RKKY) interaction [3,4], and the Kondo-lattice ground state becomes stable. Historically, these considerations have motivated a large number of path-integral mean-field treatments of the Kondo lattice [4–11] where the picture of the composite heavy fermions has been developed. One important result of these studies is that within the mean-field approximation the Fermi-surface volume expands in response to the formation of heavy electrons to accommodate the total number of occupied quasiparticle states [12].

From the experimental point of view the interest in studying the transition between large and small Fermi surfaces within the Kondo-lattice model has been mainly motivated by de Haas–van Alphen experiments where the observation of a many-body enhancement of cyclotron masses has led to the conclusion that the coherent heavy-fermion state influences all electrons and not just those with primarily f characters [13,14]. The presence of a large Fermi surface was further corroborated by measurements of the low-temperature Hall effect where a sudden collapse of the heavy-fermion state is observed near a quantum critical point [15]. An abrupt change in the Fermi surface from localized to itinerant has been confirmed by de Haas–van Alphen experiments under pressure [16].

In two dimensions and higher the Kondo-lattice model is believed to belong to the class of Fermi liquids [5,17], apart from some regions of the phase diagram [18,19]. At zero temperature, a Fermi liquid of interacting electrons has a Fermi surface, which is similar to that of noninteracting fermions. One of the most fundamental properties of Fermi liquids is Luttinger's theorem [20,21], which states that the volume inside the Fermi surface is invariant against a change in the interaction strength if the number of conduction electrons is held fixed. This requirement has remarkable consequences for the Fermi-surface properties in interacting systems as found by studies of the Friedel sum rule [22] and the Luttinger sum rule [23] for the Kondo problem. For the many-body physics in the Kondo-lattice model, the question came up whether the localized spins should be counted to the Fermi surface as electrons or not [24–26], leading either to the picture of a "large Fermi surface" as found in the mean-field treatments mentioned above or a "small Fermi surface" where conduction electrons would solely contribute to the Fermi sea volume. This question was answered by a topological proof by Oshikawa [27] who showed that localized spins in the Kondo-lattice model indeed contribute to the Fermi sea volume as electrons (in two dimensions and higher), provided the system is a Fermi liquid. Apart from the topological proof, in this paper, we show a many-body approach which can demonstrate that the Fermi sea volume is given by $\nu + 1$. Here, ν is the filling with conduction electrons, and the number 1 stands for the number of localized spins per unit cell ($S = 1/2$ and spin-symmetric case).

A theoretical approach taking into account contributions beyond the mean-field approximation has been applied to the infinite-dimensional Kondo-lattice model within the dynamical mean-field theory (DMFT). In a series of papers by Otsuki and collaborators [28,29], it was shown that for not to small Kondo coupling j_K the model is a Fermi liquid,

characterized by strong mass renormalization and a large Fermi surface. Thereby both conduction electrons and localized moments participate in the formation of the Fermi liquid, and the Luttinger volume is formed by both particle species. However, DMFT is only exactly valid for infinite dimensions and it cannot be easily extended to physical dimensions. Also the method seems not to be capable to verify the accurate value of Luttinger's theorem. Similarly, the appearance of a steplike discontinuity in the momentum distribution, found in Ref. [28], symbolizing the large Fermi surface, might be a questionable result of the DMFT. Therefore, alternative theoretical many-body methods, which are applied to the Kondo lattice in physical dimensions, are reasonable to consider.

The paper is organized as follows. In Sec. II we introduce the Kondo-lattice Hamiltonian. In Sec. III we review the basic idea of our many-body approach, called the projective renormalization method, and explain the approach to the one-particle spectral function. In Sec. IV we derive and discuss the renormalization equations for relevant parameters. The starting conditions for our numerical analysis are fixed in the beginning of Sec. V. We then show numerical results for the one-particle spectral function and momentum distribution and explain the observed features within our formalism. Finally, based on the numerical results of the previous section, we present in Sec. VI a numerical verification of Luttinger's theorem and a corresponding discussion using analytical arguments.

II. MODEL

The Kondo-lattice Hamiltonian,

$$\mathcal{H} = \sum_{\mathbf{k}\sigma} \varepsilon_{\mathbf{k}} c^{\dagger}_{\mathbf{k}\sigma} c_{\mathbf{k}\sigma} + j_K \sum_i \mathbf{S}_i \cdot \mathbf{s}_i = \mathcal{H}_0 + \mathcal{H}_1 \qquad (1)$$

describes a coupled system of conduction electrons and a periodic array of localized spins $\mathbf{S}_i$, $(S = 1/2)$ at sites i. The first term $\mathcal{H}_0$ is the kinetic energy of the conduction electrons. Here, $c^{\dagger}_{\mathbf{k}\sigma} = (1/\sqrt{N}) \sum_i c^{\dagger}_{i\sigma} \exp i\mathbf{k}\mathbf{R}_i$ is the Fourier-transformed creation operator, where $c^{(\dagger)}_{i\sigma}$ annihilates (creates) an electron with spin σ at site i. The second term $\mathcal{H}_1$ is the antiferromagnetic Kondo exchange ($j_K > 0$) between localized spin $\mathbf{S}_i$ and conduction electron spin,

$$\mathbf{s}_i = \sum_{\alpha\beta} \frac{\boldsymbol{\sigma}_{\alpha\beta}}{2} c^{\dagger}_{i\alpha} c_{i\beta}, \qquad (2)$$

and $\boldsymbol{\sigma}_{\alpha\beta}$ is the vector Pauli matrix. Note that the Kondo exchange $\mathcal{H}_1$ prevents the direct solution of the model through the presence of transitions between the different eigenstates of $\mathcal{H}_0$.

III. METHOD

Let us start from a short review of the projective renormalization method (PRM) [30]. The PRM is a novel renormalization scheme in which the renormalization process is implemented in the Liouville space (that is built up by all operators of the Hilbert space). The basic idea of the PRM is to integrate out the interaction $\mathcal{H}_1$ by a series of small unitary transformations starting from large-to-zero transition energies. Assuming that all transitions with transition energies higher than some energy cutoff λ have already been integrated out, the transformed Hamiltonian will be denoted by $\mathcal{H}_\lambda$. The transformation of $\mathcal{H}_\lambda$ to a new renormalized $\mathcal{H}_{\lambda-\Delta\lambda}$ with a slightly reduced energy cutoff $\lambda - \Delta\lambda$ is formally obtained by

$$\mathcal{H}_{\lambda-\Delta\lambda} = e^{X_{\lambda,\Delta\lambda}} \mathcal{H}_\lambda e^{-X_{\lambda,\Delta\lambda}}, \qquad (3)$$

where $X_{\lambda,\Delta\lambda} = -X^{\dagger}_{\lambda,\Delta\lambda}$ is the generator of the unitary transformation. It is fixed by the requirement that $\mathcal{H}_{\lambda-\Delta\lambda}$ no longer contains excitations with energies higher than $\lambda - \Delta\lambda$. Explicit evaluation of the unitary transformation leads to discrete renormalization equations, which connect the parameters of $\mathcal{H}_{\lambda-\Delta\lambda}$ with those of $\mathcal{H}_\lambda$. The complete elimination procedure starts from the parameter values of the original model (1) and proceeds in small steps $\Delta\lambda$ until $\lambda = 0$ is reached. Then all transitions from $\mathcal{H}_1$ are used up, i.e., in the fully renormalized Hamiltonian $\tilde{\mathcal{H}} := \mathcal{H}_{\lambda=0}$ the perturbation $\mathcal{H}_1$ is completely integrated out.

Note that the PRM resembles alternative renormalization methods developed independently by Głazek and Wilson [31,32] and Kehrein [33] and by Wegner and co-workers [34], which are also based on the application of unitary transformations. Thereby as in the PRM, no states are eliminated. Instead, the basic states are changed in such a way that the renormalized Hamiltonian, which was called $\mathcal{H}_\lambda$ in the PRM, only includes states with unperturbed energy differences smaller than some chosen energy cutoff λ. However, there is a difference between these methods. During the renormalization procedure of the PRM the interaction $\mathcal{H}_1$ is successively integrated out in small energy steps $\Delta\lambda$ between λ and $\lambda - \Delta\lambda$. That is, only states with excitation energies within the respective energy interval $\Delta\lambda$ are eliminated in each step. In contrast, in the so-called "similarity renormalization group" by Głazek and Wilson [31,32] and Kehrein [33] and similarly in "the flow equation method" by Wegner and co-workers [34], all states with energy differences smaller than λ and not only within the interval $\Delta\lambda$ are involved in each elimination step. However, in order to obtain thereby an increasingly diagonal Hamiltonian matrix an appropriate unitary transformation has to be chosen by hand, which implies an additional choice for an appropriate unitary transformation. In contrast, the unitary transformation in the PRM is fixed by the above-mentioned rules although the generators of the transformations of Głazek and Wilson and Wegner and co-workers may be included in the PRM [35] as well. Finally, one should mention that Wegner's flow equation method is a continuous version of the renormalization approach where the width of the integration steps has approached zero.

In actual calculations using the PRM the total number of renormalization steps $\Delta\lambda$ should be very large, i.e., on the order of the particle number. Therefore, the width $\Delta\lambda$ of each small renormalization step is very small, which allows using perturbation theory in $\mathcal{H}_1$ in each renormalization step. To be more specific in this point, the number of renormalization processes in each energy step $\Delta\lambda$ due to $\mathcal{H}_1$ has to be small compared to the total number of such processes. Thus, roughly speaking, the "smallness parameter" for the present perturbative treatment is not simply the strength of the perturbation $\mathcal{H}_1$ compared to the energy scale of $\mathcal{H}_0$. Instead this ratio is multiplied by the number of renormalization

processes inside the shell $\Delta\lambda$ compared to their total number. Therefore, perturbation theory in each renormalization step is usually allowed. The overall renormalization procedure down to $\lambda = 0$ is valid far beyond usual perturbation theory since renormalization processes to infinite order in $\mathcal{H}_1$ are taken into account.

In Ref. [36] the following *ansatz* was shown to be an appropriate choice for the transformed Kondo Hamiltonian $\mathcal{H}_\lambda$ at cutoff λ,

$$\mathcal{H}_\lambda = \mathcal{H}_{0,\lambda} + \mathcal{H}_{1,\lambda}, \tag{4}$$

with

$$\mathcal{H}_{0,\lambda} = \sum_{\mathbf{k}\sigma} \varepsilon_{\mathbf{k},\lambda} c^\dagger_{\mathbf{k}\sigma} c_{\mathbf{k}\sigma} + \sum_{\mathbf{q}} J_{\mathbf{q},\lambda} \mathbf{S}_{\mathbf{q}} \cdot \mathbf{S}_{-\mathbf{q}} + E_\lambda, \tag{5}$$

$$\mathcal{H}_{1,\lambda} = \frac{1}{\sqrt{N}} \sum_{\mathbf{k}\mathbf{k}'} j_{\mathbf{k}'\mathbf{k},\lambda} \Theta_{\mathbf{k}'\mathbf{k},\lambda} \mathcal{K}_{\mathbf{k}'\mathbf{k}}. \tag{6}$$

The Θ-function $\Theta_{\mathbf{k}'\mathbf{k},\lambda} = \Theta(\lambda - |\varepsilon_{\mathbf{k}',\lambda} - \varepsilon_{\mathbf{k},\lambda}|)$ in Eq. (6) limits the excitations to energies smaller than λ and $\mathcal{K}_{\mathbf{k}'\mathbf{k}}$ results from the decomposition of $\mathcal{H}_1$ into dynamical eigenvectors of $\mathcal{H}_{0,\lambda}$,

$$\mathcal{K}_{\mathbf{k}'\mathbf{k}} = \frac{1}{2} \sum_{\alpha\beta} \mathbf{S}_{\mathbf{k}'-\mathbf{k}} \cdot \boldsymbol{\sigma}_{\alpha\beta} c^\dagger_{\mathbf{k}\alpha} c_{\mathbf{k}'\beta}. \tag{7}$$

Moreover, a $\mathbf{k}$ dependence in the Kondo coupling $j_{\mathbf{k}'\mathbf{k},\lambda}$ was generated by transformation (3) as well as an effective RKKY exchange interaction between localized spins $\mathbf{S}_i$ and $\mathbf{S}_j$. E_λ is an additional energy shift. As already anticipated, all parameters of $\mathcal{H}_\lambda$ depend on the cutoff λ. Note that $\mathcal{H}_\lambda$ reduces to the original Hamiltonian $\mathcal{H}$ for the initial parameters,

$$\varepsilon_{\mathbf{k},\Lambda} = \varepsilon_{\mathbf{k}}, \quad J_{\mathbf{q},\Lambda} = 0, \quad E_\Lambda = 0, \quad j_{\mathbf{k}'\mathbf{k},\Lambda} = j_K, \tag{8}$$

where $\lambda = \Lambda$ is the cutoff of the original model (1).

According to Ref. [36] the generator $X_{\lambda,\Delta\lambda}$ of transformation (3) is given to lowest order in $j_{\mathbf{k}'\mathbf{k},\lambda}$ by

$$X_{\lambda,\Delta\lambda} = \frac{1}{\sqrt{N}} \sum_{\mathbf{k}\mathbf{k}'} X_{\mathbf{k}'\mathbf{k}}(\lambda, \Delta\lambda) \mathcal{K}_{\mathbf{k}'\mathbf{k}}, \tag{9}$$

with

$$X_{\mathbf{k}'\mathbf{k}}(\lambda, \Delta\lambda) = \frac{j_{\mathbf{k}'\mathbf{k},\lambda}}{\varepsilon_{\mathbf{k}',\lambda} - \varepsilon_{\mathbf{k},\lambda}} \Theta_{\mathbf{k}'\mathbf{k},\lambda} (1 - \Theta_{\mathbf{k}'\mathbf{k},\lambda-\Delta\lambda}). \tag{10}$$

$X_{\lambda,\Delta\lambda}$ is fixed by the requirement that $\mathcal{H}_{\lambda-\Delta\lambda}$ no longer contains excitations with energies higher than $\lambda - \Delta\lambda$. Evaluating the unitary transformation to order $j^2_{\mathbf{k}\mathbf{k}',\lambda}$ discrete renormalization equations for the parameters $\varepsilon_{\mathbf{k},\lambda}$, $J_{\mathbf{q},\lambda}$, E_λ, and $j_{\mathbf{k}'\mathbf{k},\lambda}$ are obtained which connect the parameters at cutoff λ with those at $\lambda - \Delta\lambda$. As above mentioned, the complete elimination procedure starts from the parameter values (8) of the original model (1) and proceeds in steps $\Delta\lambda$ until $\lambda = 0$ is reached. Then all transitions from $\mathcal{H}_1$ are used up, and the fully renormalized Hamiltonian $\tilde{\mathcal{H}} := \mathcal{H}_{\lambda=0} = \mathcal{H}_{0,\lambda=0}$ reads

$$\tilde{\mathcal{H}} = \sum_{\mathbf{k}\sigma} \tilde{\varepsilon}_{\mathbf{k}} c^\dagger_{\mathbf{k}\sigma} c_{\mathbf{k}\sigma} + \tilde{\mathcal{H}}_J + \tilde{E}, \tag{11}$$

with

$$\tilde{\mathcal{H}}_J = \sum_{\mathbf{q}} \tilde{J}_{\mathbf{q}} \mathbf{S}_{\mathbf{q}} \cdot \mathbf{S}_{-\mathbf{q}}. \tag{12}$$

Here, $\tilde{\varepsilon}_{\mathbf{k}}$, $\tilde{J}_{\mathbf{q}}$, and $\tilde{E}$ are the fully renormalized quantities. Note that expression (11) describes an uncoupled system of conduction electrons and localized spins.

The fully renormalized Hamiltonian $\tilde{\mathcal{H}}$ can be used to calculate physical quantities. This follows from the property that any operator below a trace is invariant under unitary transformations. Applied to the one-particle spectral function $A(\mathbf{k}, \omega) = (1/2\pi) \int_{-\infty}^{\infty} \langle [c_{\mathbf{k}\sigma}(t), c^\dagger_{\mathbf{k}\sigma}]_+ \rangle e^{i\omega t} dt$, this property immediately leads to

$$A(\mathbf{k}, \omega) = \frac{1}{2\pi} \int_{-\infty}^{\infty} \langle [\tilde{c}_{\mathbf{k}\sigma}(t), \tilde{c}^\dagger_{\mathbf{k}\sigma}]_+ \rangle_{\tilde{\mathcal{H}}} e^{i\omega t} dt. \tag{13}$$

Now both the time dependence and the expectation value are formed with $\tilde{\mathcal{H}}$. The quantity $\tilde{c}^\dagger_{\mathbf{k}\sigma} = c^\dagger_{\mathbf{k}\sigma}(\lambda = 0)$ is the transformed one-particle operator. Here, $c^\dagger_{\mathbf{k}\sigma}(\lambda) = e^{X_\lambda} c^\dagger_{\mathbf{k}\sigma} e^{-X_\lambda}$, which has the operator structure,

$$c^\dagger_{\mathbf{k}\sigma}(\lambda) = u_{\mathbf{k},\lambda} c^\dagger_{\mathbf{k}\sigma} + \frac{1}{\sqrt{N}} \sum_{\mathbf{k}'} v_{\mathbf{k}'\mathbf{k},\lambda} \mathcal{D}^\dagger_{\mathbf{k}\sigma;\mathbf{k}'}, \tag{14}$$

with

$$\mathcal{D}^\dagger_{\mathbf{k}\sigma;\mathbf{k}'} = \sum_{\alpha} \mathbf{S}_{\mathbf{k}-\mathbf{k}'} \cdot \frac{\boldsymbol{\sigma}_{\alpha\sigma}}{2} c^\dagger_{\mathbf{k}'\alpha}. \tag{15}$$

Similar to $\mathcal{H}_\lambda$ [Eq. (4)] the operator structure (14) follows from a low coupling expansion of $c^\dagger_{\mathbf{k}\sigma}(\lambda)$. The initial conditions of the λ-dependent coefficients are

$$u_{\mathbf{k},\Lambda} = 1, \quad v_{\mathbf{k}'\mathbf{k},\Lambda} = 0,$$

where $\lambda = \Lambda$ is again the cutoff energy of the original model. Neglecting in Eq. (13) the influence of the spin interaction $\tilde{\mathcal{H}}_J$ on the dynamics of $\tilde{c}_{\mathbf{k}\sigma}(t)$ one immediately finds

$$A(\mathbf{k}, \omega) = |\tilde{u}_{\mathbf{k}}|^2 \delta(\omega - \tilde{\varepsilon}_{\mathbf{k}}) + \frac{1}{4N} \sum_{\mathbf{k}'} |\tilde{v}_{\mathbf{k}'\mathbf{k}}|^2 S^J(\mathbf{k}' - \mathbf{k}) \delta(\omega - \tilde{\varepsilon}_{\mathbf{k}'}), \tag{16}$$

where $S^J(\mathbf{k}' - \mathbf{k})$ is the spin-correlation function formed with the fully renormalized Hamiltonian $\tilde{\mathcal{H}}$,

$$S^J(\mathbf{k}' - \mathbf{k}) = \langle \mathbf{S}_{\mathbf{k}'-\mathbf{k}} \cdot \mathbf{S}_{\mathbf{k}-\mathbf{k}'} \rangle_{\tilde{\mathcal{H}}}. \tag{17}$$

IV. RENORMALIZATION EQUATIONS FOR $u_{\mathbf{k},\lambda}$ AND $v_{\mathbf{k}'\mathbf{k},\lambda}$

Next the renormalization equations for the parameters $u_{\mathbf{k},\lambda}$ and $v_{\mathbf{k}'\mathbf{k},\lambda}$ are needed. According to the Appendix, one finds

$$u_{\mathbf{k},\lambda-\Delta\lambda} - u_{\mathbf{k},\lambda} = -\frac{1}{8N} \sum_{\mathbf{k}'} [u_{\mathbf{k},\lambda} X_{\mathbf{k}'\mathbf{k}}(\lambda, \Delta\lambda) + 2 v_{\mathbf{k}'\mathbf{k},\lambda}] \times X_{\mathbf{k}'\mathbf{k}}(\lambda, \Delta\lambda) S(\mathbf{k}' - \mathbf{k}) + \frac{1}{4N^{3/2}} \times \sum_{\mathbf{k}'\mathbf{q}} [u_{\mathbf{k},\lambda} X_{\mathbf{k}'\mathbf{k}}(\lambda, \Delta\lambda) + 2 v_{\mathbf{k}'\mathbf{k},\lambda}] \times X_{\mathbf{q}\mathbf{k}}(\lambda, \Delta\lambda) \langle \mathcal{K}_{\mathbf{k}'\mathbf{q}} \rangle, \tag{18}$$

and

$$v_{\mathbf{k}'\mathbf{k},\lambda-\Delta\lambda} - v_{\mathbf{k}'\mathbf{k},\lambda} = u_{\mathbf{k},\lambda} X_{\mathbf{k}'\mathbf{k}}(\lambda, \Delta\lambda) + \frac{1}{4N} \times \sum_{\mathbf{q}} [u_{\mathbf{k},\lambda} X_{\mathbf{q}\mathbf{k}}(\lambda, \Delta\lambda) + 2v_{\mathbf{q}\mathbf{k},\lambda}] \times X_{\mathbf{k}'\mathbf{q}}(\lambda, \Delta\lambda)[2\langle c^\dagger_{\mathbf{q}\alpha} c_{\mathbf{q}\alpha}\rangle - 1]. \quad (19)$$

In Eq. (18) the spin-correlation function $S(\mathbf{k}' - \mathbf{k})$ is formed with the original Hamiltonian $\mathcal{H}$ and not with $\tilde{\mathcal{H}}$ as before

$$S(\mathbf{k}' - \mathbf{k}) = \langle \mathbf{S}_{\mathbf{k}'-\mathbf{k}} \cdot \mathbf{S}_{\mathbf{k}-\mathbf{k}'} \rangle. \quad (20)$$

Note that in the heavy-fermion regime the spin correlations between different sites are small [37,38] so that $S(\mathbf{k}' - \mathbf{k})$ is almost wave-vector independent and can be replaced by its single-site value. Therefore, we set for simplicity $S(\mathbf{k}' - \mathbf{k}) \approx S(S+1) \approx S^J(\mathbf{k}' - \mathbf{k})$.

Let us first study the properties of Eq. (18). This equation contains two renormalization contributions on the right-hand side. Taking advantage of the fact that $u_{\mathbf{k},\lambda} \geqslant 0$ and $S(\mathbf{k}' - \mathbf{k}) > 0$, one finds that the first contribution is always negative and tends to decrease the parameter $u_{\mathbf{k},\lambda}$. Thereby one has used that $v_{\mathbf{k}'\mathbf{k},\lambda}$ has the same sign as $X_{\mathbf{k}'\mathbf{k}}(\lambda, \Delta\lambda)$. Similarly, also the second term of Eq. (18) is negative since $\langle \mathcal{K}_{\mathbf{k}'\mathbf{q}} \rangle$ is always negative. This quantity indicates the formation of the singlet state [36]. It strongly decreases to large negative values with decreasing temperature for wave-vectors $\mathbf{k}' \approx \mathbf{q} \approx \mathbf{k}_F$. Thus, in the renormalization procedure both renormalization contributions of Eq. (18) tend to reduce $u_{\mathbf{k},\lambda}$ thereby starting from its initial value of 1. The fully renormalized quantity $\tilde{u}_{\mathbf{k}}$ should vanish, which is verified by the explicit solution of Eqs. (18) and (19).

Thus, only the second part $\sim |\tilde{v}_{\mathbf{k}'\mathbf{k}}|^2$ of expression (16) for $A(\mathbf{k}, \omega)$ survives, and the spectral function reduces to

$$A(\mathbf{k}, \omega) = \frac{S(S+1)}{4N} \sum_{\mathbf{k}'} |\tilde{v}_{\mathbf{k}'\mathbf{k}}|^2 \delta(\omega - \tilde{\varepsilon}_{\mathbf{k}'}). \quad (21)$$

Note that the remaining coefficients $\tilde{v}_{\mathbf{k}'\mathbf{k}}$ in Eq. (21) obey the following sum rule for any $\mathbf{k}$:

$$1 = \frac{S(S+1)}{4N} \sum_{\mathbf{k}'} |\tilde{v}_{\mathbf{k}'\mathbf{k}}|^2, \quad (22)$$

which follows from the anticommutator relation $\int d\omega\, A(\mathbf{k}, \omega) = \langle [c^\dagger_{\mathbf{k},\sigma}, c_{\mathbf{k}\sigma}]_+ \rangle = 1$. To find $A(\mathbf{k}, \omega)$ the renormalized frequencies $\tilde{\varepsilon}_{\mathbf{k}'}$ and the coefficients $\tilde{v}_{\mathbf{k}'\mathbf{k}}$ must be evaluated.

The momentum distribution $\langle c^\dagger_{\mathbf{k}\alpha} c_{\mathbf{k}\alpha} \rangle$, which enters Eq. (19), is related to the single-particle spectral function $A(\mathbf{k}, \omega)$ via the fluctuation-dissipation theorem,

$$\langle c^\dagger_{\mathbf{k}\alpha} c_{\mathbf{k}\alpha} \rangle = \int_{-\infty}^{\infty} \frac{A(\mathbf{k}, \omega)}{1 + e^{\beta\omega}} d\omega = \frac{S(S+1)}{4N} \sum_{\mathbf{k}'} |\tilde{v}_{\mathbf{k}'\mathbf{k}}|^2 f(\tilde{\varepsilon}_{\mathbf{k}'}), \quad (23)$$

where $f(\tilde{\varepsilon}_{\mathbf{k}'}) = 1/(1 + e^{\beta\tilde{\varepsilon}_{\mathbf{k}'}})$ is the Fermi function. At zero-temperature $T = 0$ only energies $\tilde{\varepsilon}_{\mathbf{k}'}$ below the Fermi surface contribute to the sum over $\mathbf{k}'$.

V. NUMERICAL RESULTS

In the actual evaluation of the renormalization equations, we restrict ourselves to a two-dimensional square lattice ($d = 2$) with $N = 10^3$ lattice points in order to minimize the numerical effort. Also, we consider only electron concentrations ν away from half-filling since in the specific half-filled case the system becomes insulating. Here, we define $\nu = (2/N) \sum_{\mathbf{k}<\mathbf{k}_F^S} 1$ for the filling of a free conduction electron system with both spin directions included. Here, $\mathbf{k}_F^S$ is the corresponding Fermi momentum as specified below. For the initial dispersion $\varepsilon_{\mathbf{k}}$ of the free system we consider an isotropic parabolic band $\varepsilon_{\mathbf{k}} = -2t(1 - k^2) - \mu$, where μ is the chemical potential and t is the nearest-neighbor hopping matrix element. Using chosen values for the two initial parameters j_K/t and ν (which is fixed by μ/t) we solve the system of Eqs. (18), (19), and (23) self-consistently. Finally, these results are used to calculate the one-particle spectral function $A(\mathbf{k}, \omega)$ from Eq. (21) and particle numbers from Eq. (23).

A. Single-particle spectrum

Figure 1 shows the one-particle spectral function $A(\mathbf{k}, \omega)$ as a function of ω for various $\mathbf{k}$ values around the Fermi momentum k_F^S between $k_F^S - \pi/10$ and $k_F^S + \pi/10$. Here, k_F^S is the Fermi momentum of the free conduction electron system (small Fermi surface) as defined by $-2t[1 - (k_F^S)^2] - \mu = 0$.

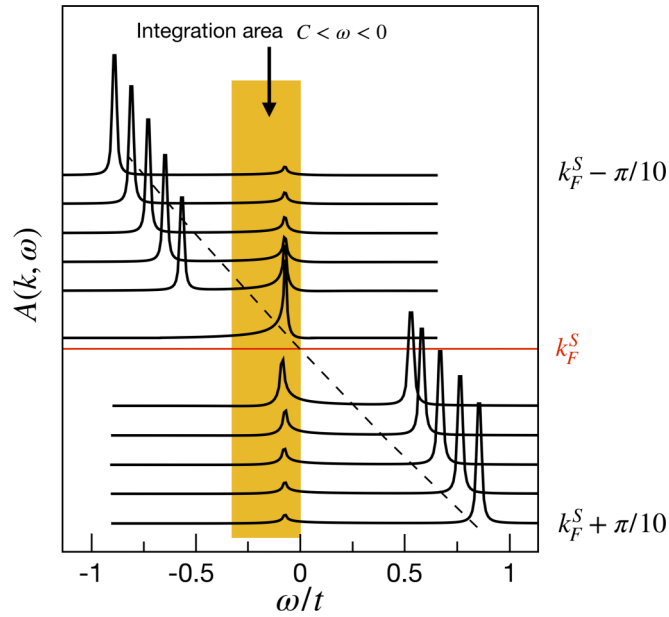

FIG. 1. Spectral function $A(\mathbf{k}, \omega)$ versus ω for $T = 0$, $j_K/t = 0.3$, and $\nu = 0.22$. Shown are several curves for different $\mathbf{k}$ values in the region between $k_F^S - \pi/10$ and $k_F^S + \pi/10$ around the Fermi momentum k_F^S of the small Fermi surface. The nearly dispersionless Kondo resonance (orange shaded area) appears slightly below the Fermi energy $\omega = 0$ and is clearly separated from the coherent excitations which follow the dispersion of the renormalized conduction electron band $\tilde{\varepsilon}_{\mathbf{k}}$, slightly deviating from the original dispersion $\varepsilon_{\mathbf{k}}$ (dashed line). The orange area highlights the energy integration interval $C < \omega < 0$ which is used to define the different contributions to the total particle number in Eq. (35).

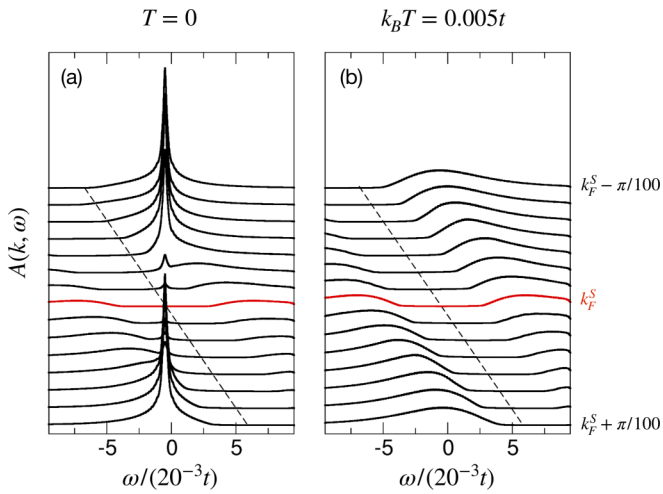

FIG. 2. Spectral function $A(\mathbf{k}, \omega)$ as in Fig. 1 but for the two temperatures $T = 0$ and $T = 0.005t$ in a very narrow region around the Fermi momentum $\mathbf{k}_F^S$ of the small Fermi surface between $\mathbf{k}_F^S - \pi/100$ and $\mathbf{k}_F^S + \pi/100$. Whereas the Kondo resonance is clearly seen for $T = 0$, it has disappeared for $T = 5 \times 10^{-3}t$ which is larger than the Kondo temperature.

The parameters are $j_K/t = 0.3$ and $\nu = 0.22$. Clearly seen is the coherent one-particle excitation of the conduction electrons which follows the slightly renormalized dispersion $\tilde{\varepsilon}_\mathbf{k}$. The initial dispersion $\varepsilon_\mathbf{k}$, which crosses the Fermi level at $\omega = 0$, is indicated by a dashed line. Moreover, an additional almost $\mathbf{k}$-independent excitation is found at an energy $\varepsilon_{\text{Kondo}} < 0$ slightly below the Fermi level (orange shaded area). This excitation has to be interpreted as Kondo resonance. Note that the intensity of the Kondo resonance decreases with increasing values of $\mathbf{k}$ away from $\mathbf{k}_F^S$ until it completely disappears for larger values of $\mathbf{k}$. Here, only the coherent excitation far away from the Fermi energy survives. Vice versa, for $\mathbf{k}$ values very close to $\mathbf{k}_F^S$ only the Kondo excitations remains, whereas the coherent excitation is absent.

This feature is even better seen in Fig. 2(a) where the spectral function $A(\mathbf{k}, \omega)$ is shown in a much smaller $\mathbf{k}$ regime around $\mathbf{k}_F^S$ only. Here only the Kondo excitation is found, whereas the dispersive excitation ($\varepsilon_\mathbf{k}$ again indicated by a dashed line) is completely absent. Note that in the immediate vicinity of $\mathbf{k}_F^S$ (in a range of $10^{-3}\pi$) the Kondo resonance has dissipated in a rather broad and incoherent spectrum. In the right panel of Fig. 2 the spectral function is shown for an increased temperature of $T = 5 \times 10^{-3}t$ which is above the Kondo temperature of $T_K \approx 5 \times 10^{-4}t$. In this case, the Kondo resonance is not found anymore.

The Kondo resonance always remains slightly below the Fermi energy. In particular, it does not cross the Fermi energy at some larger $\mathbf{k}_F^L$ as is claimed in Ref. [28]. Instead, in the present approach, the Kondo resonance loses its strength with increasing distance from $\mathbf{k}_F^S$ which is essential for the validity of Luttinger's theorem. In particular, this property leads to the existence of a large Fermi surface which is composed of dispersive and Kondo resonance excitations. Thereby, the dispersionless Kondo excitation appears as a resonancelike feature slightly below the Fermi level and is rather smoothly connected to the coherent excitation of the conduction

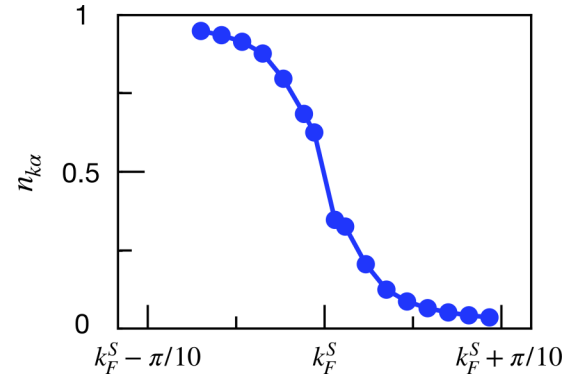

FIG. 3. Momentum distribution $n_{\mathbf{k}\alpha} = \langle c_{\mathbf{k}\sigma}^\dagger c_{\mathbf{k}\sigma} \rangle$ plotted versus $\mathbf{k}$ around the Fermi momentum $\mathbf{k}_F^S$ for $T = 0$ and the same parameters as in Fig. 1. Note that the shape of $\langle c_{\mathbf{k}\sigma}^\dagger c_{\mathbf{k}\sigma} \rangle$ differs from that of free conduction electrons due to the presence of the Kondo exchange.

electrons. Note that the overall shape of $A(\mathbf{k}, \omega)$ in Fig. 1 is consistent with mean-field theory and DMFT studies of the Kondo-lattice model. However, in the present paper the Kondo effect does not result from hybridization effects between c and f electrons but from a many-body effect between coherent excitations and localized spins thereby avoiding any reduction to a single-particle description. Nevertheless, as we will show below, our theory perfectly fulfills Luttinger's theorem for the Kondo-lattice model and is therefore fully consistent with the well-accepted concept of the large Fermi surface.

B. Momentum distribution $n_{\mathbf{k}\alpha}$

To prepare the study of Luttinger's theorem within our approach let us at first consider the properties of the momentum distribution $n_{\mathbf{k}\alpha} = \langle c_{\mathbf{k}\alpha}^\dagger c_{\mathbf{k}\alpha} \rangle$. For this one again needs the renormalized coefficients $\tilde{v}_{\mathbf{k}'\mathbf{k}}$. As aforementioned, they follow from the solution of Eq. (18) which also depends on $\langle c_{\mathbf{k}\alpha}^\dagger c_{\mathbf{k}\alpha} \rangle$.

Figure 3 shows the result for $n_{\mathbf{k}\alpha}$ for temperature $T = 0$ and the same parameters as in Fig. 1. As expected, $n_{\mathbf{k}\alpha}$ differs from the usual Fermi function for free particles. Thereby, the steplike behavior at the Fermi-level ε_F is replaced in Fig. 3 by a gradual decay. Only for large negative and large positive values of $\tilde{\varepsilon}_\mathbf{k}$ away from the Fermi surface the momentum distribution approaches the values of 1 and 0 as for free conduction electrons. Such behavior is qualitatively consistent with other numerical work (for example, Ref. [28]). However, in contrast to Ref. [28] and mean-field approaches, we here do not find a steplike behavior of the occupation number at some large Fermi momentum $\mathbf{k}_F^L$. Instead, a rather smooth decrease down to zero is obtained within the PRM approach.

C. Discussion

Now we are in the position to discuss the origin of the ω structure of $A(\mathbf{k}, \omega)$. One best starts from the renormalization equation (19) for $v_{\mathbf{k}'\mathbf{k},\lambda}$. First, note that the second term in Eq. (19) becomes large if $\mathbf{k}'$ is located close to $\mathbf{k}_F^S$ (i.e., if $\varepsilon_{\mathbf{k}'} \approx \varepsilon_F^S$) and with rather arbitrary values of $\mathbf{k} \neq \mathbf{k}_F^S$. Here, one uses the fact that the renormalization of $\tilde{\varepsilon}_\mathbf{k}$ is small and the momentum distribution $\langle c_{\mathbf{q}\alpha}^\dagger c_{\mathbf{q}\alpha} \rangle$ is such as shown in

Fig. 3. Then, in the internal sum over $\mathbf{q}$ of Eq. (19) the factor $(2\langle c^\dagger_{\mathbf{q}\alpha} c_{\mathbf{q}\alpha}\rangle - 1)$ softly decreases as a function of $\tilde{\varepsilon}_\mathbf{q}$ from 1 far below ε_F to (-1) far above ε_F. Thereby the factor crosses the Fermi energy at ε_F. Taking, moreover, the diverging character of $X_{\mathbf{k}'\mathbf{q}}(\lambda, \Delta\lambda)$ at $\tilde{\varepsilon}_\mathbf{q} \approx \tilde{\varepsilon}_{\mathbf{k}'}$ into account one easily assures oneself that the $\mathbf{q}$ sum becomes largest for $\varepsilon_{\mathbf{k}'}$ located closely below the Fermi level. Thus, the fully renormalized coefficient $\tilde{v}_{\mathbf{k}'\mathbf{k}}$ has a maximum at an energy $\varepsilon_{\text{Kondo}}$ slightly below ε_F. Thereby we have restricted ourselves to $T = 0$ where in the internal sum (23) of the momentum distribution $\langle c^\dagger_{\mathbf{q}\alpha} c_{\mathbf{q}\alpha}\rangle$ only wave-vectors $\mathbf{k}'$ contribute to $\tilde{v}_{\mathbf{k}'\mathbf{q}}$ which have negative energies $\tilde{\varepsilon}_{\mathbf{k}'} < 0$. This property of $\tilde{v}_{\mathbf{k}'\mathbf{k}}$ explains the Kondo resonance in Figs. 1 or 2. The $\mathbf{k}$ dependence of the Kondo resonance is caused by the additional factor of $X_{\mathbf{q}\mathbf{k}}(\lambda, \Delta\lambda)$ in the sum over $\mathbf{q}$ in Eq. (19). Together with the factor of $X_{\mathbf{k}'\mathbf{q}}(\lambda, \Delta\lambda)$ it is responsible for the observed decrease in the Kondo resonance intensity if the distance between $\varepsilon_\mathbf{k}$ and $\varepsilon_{\mathbf{k}'}$ is increased. This follows from the structure (10) of $X_{\mathbf{k}'\mathbf{k}}(\lambda, \Delta\lambda)$ which shows that the product of $X_{\mathbf{q}\mathbf{k}}(\lambda, \Delta\lambda) X_{\mathbf{k}'\mathbf{q}}(\lambda, \Delta\lambda)$ becomes weaker when the distance is increased.

However, there is a second renormalization contribution to $v_{\mathbf{k}'\mathbf{k},\lambda}$ which becomes important. This is the case when $\varepsilon_{\mathbf{k}',\lambda}$ and $\varepsilon_{\mathbf{k},\lambda}$ are close to each other ($\tilde{\varepsilon}_{\mathbf{k}'} \approx \tilde{\varepsilon}_\mathbf{k}$). Then the first term $u_{\mathbf{k},\lambda} X_{\mathbf{k}'\mathbf{k}}(\lambda, \Delta\lambda)$ on the right-hand side of Eq. (19) increases during the renormalization procedure.

To sum up, there are two main contributions to $\tilde{v}_{\mathbf{k}'\mathbf{k}}$. One results from $\tilde{\varepsilon}_{\mathbf{k}'} \approx \varepsilon_F$, and $\tilde{\varepsilon}_\mathbf{k}$ is rather arbitrary. The other one occurs for $\tilde{\varepsilon}_{\mathbf{k}'} \approx \tilde{\varepsilon}_\mathbf{k}$. Thereby the first one leads to Kondo excitations, whereas the second one should be related to the dispersive excitations in Fig. 2. Combining both contributions, we are led to the following approximate decomposition of $A(\mathbf{k}, \omega)$:

$$A(\mathbf{k}, \omega) \approx \frac{S(S+1)}{4N} \sum_{\mathbf{k}'}^{\tilde{\varepsilon}_{\mathbf{k}'} (\approx \varepsilon_{\text{Kondo}})} |\tilde{v}_{\mathbf{k}'\mathbf{k}}|^2 \delta(\omega - \tilde{\varepsilon}_{\mathbf{k}'}) + \frac{S(S+1)}{4N} \sum_{\mathbf{k}'}^{\tilde{\varepsilon}_{\mathbf{k}'} (\approx \tilde{\varepsilon}_\mathbf{k})} |\tilde{v}_{\mathbf{k}'\mathbf{k}}|^2 \delta(\omega - \tilde{\varepsilon}_\mathbf{k}). \quad (24)$$

The first term describes almost dispersionless excitations at energies $\tilde{\varepsilon}_{\mathbf{k}'} (\approx \varepsilon_{\text{Kondo}})$ leading to the Kondo resonance. Only the $\mathbf{k}$ dependence of $\tilde{v}_{\mathbf{k}'\mathbf{k}}$ causes the $\mathbf{k}$-dependent decrease in its intensity as mentioned above. The second term in Eq. (24) must generate the single-particle excitations since the coefficient $\tilde{u}_\mathbf{k}$ of the original dispersive excitation in Eq. (16) had vanished before ($\tilde{u}_\mathbf{k} = 0$). To prove this statement, we apply the sum rule $\int d\omega\, A(\mathbf{k}, \omega) = 1$ to Eq. (24) and obtain

$$1 \approx \frac{S(S+1)}{4N} \sum_{\mathbf{k}'}^{\tilde{\varepsilon}_{\mathbf{k}'} (\approx \varepsilon_{\text{Kondo}})} |\tilde{v}_{\mathbf{k}'\mathbf{k}}|^2 + \frac{S(S+1)}{4N} \sum_{\mathbf{k}'}^{\tilde{\varepsilon}_{\mathbf{k}'} (\approx \tilde{\varepsilon}_\mathbf{k})} |\tilde{v}_{\mathbf{k}'\mathbf{k}}|^2. \quad (25)$$

From the former discussion in Sec. IV it becomes clear that the amplitude $|\tilde{v}_{\mathbf{k}'\mathbf{k}}|^2$ of the first term becomes increasingly small when $\tilde{\varepsilon}_\mathbf{k}$ is energetically well separated from the Kondo excitations $\tilde{\varepsilon}_{\mathbf{k}'} \approx \varepsilon_{\text{Kondo}}$. Thus, Eq. (25) reduces for large $|\tilde{\varepsilon}_\mathbf{k}|$

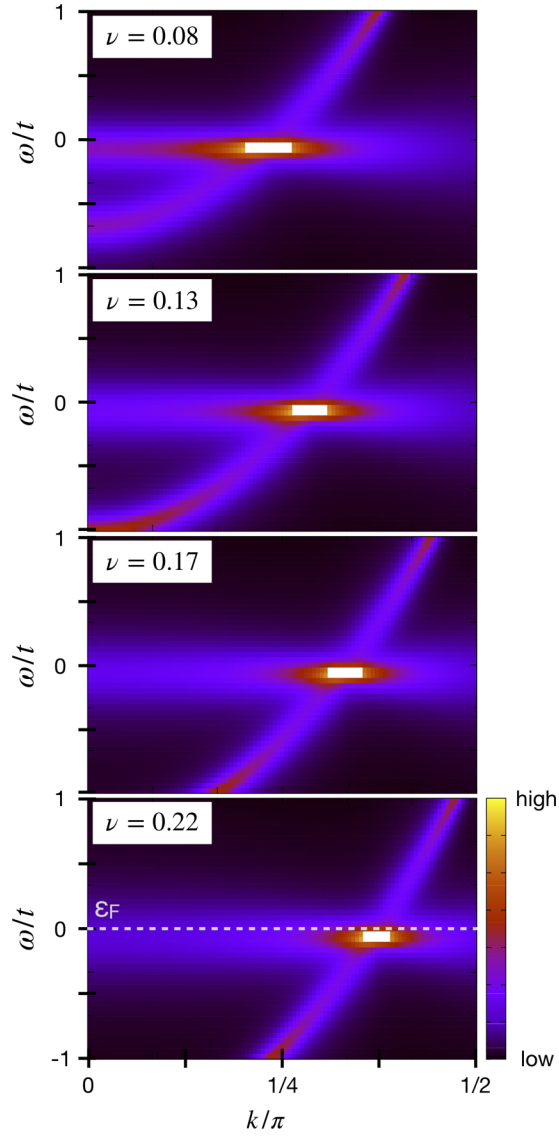

FIG. 4. Spectral function $A(\mathbf{k}, \omega)$ at $T = 0$ in a wide momentum and energy range for different filling values ν. The Kondo resonance always appears slightly below the Fermi level (dashed line) and has its maximum intensity in a narrow momentum region around the Fermi momentum k_F^S of the small Fermi surface (the white color means an exaggerated intensity beyond the scale of the color bar). Away from k_F^S the intensity of the Kondo resonance decays like $\propto 1/k$ and therefore appears in a wide momentum region (purple and red colors). This behavior is nearly independent of ν.

to

$$1 \approx \frac{S(S+1)}{4N} \sum_{\mathbf{k}'}^{\tilde{\varepsilon}_{\mathbf{k}'} (\approx \tilde{\varepsilon}_\mathbf{k})} |\tilde{v}_{\mathbf{k}'\mathbf{k}}|^2. \quad (26)$$

Comparison with Eq. (24) shows that the right-hand side of Eq. (26) represents the amplitude of the dispersive excitation part in $A(\mathbf{k}, \omega)$. Therefore, $A(\mathbf{k}, \omega)$ reduces for large $|\tilde{\varepsilon}_\mathbf{k}|$ to

$$A(\mathbf{k}, \omega)|_{\text{c,el}} \approx \delta(\omega - \tilde{\varepsilon}_\mathbf{k}), \quad (27)$$

which is the spectral function of free conduction electrons. This behavior is also clearly seen in Fig. 4 where for different

chosen filling values always a sharp excitation with single-particle character is found far below and above the Fermi level. This nearly free-particle excitation appears for most of the $\mathbf{k}$ vectors energetically well separated from the dispersionless Kondo excitation close to the Fermi level. One concludes that both the Kondo resonance and the one-particle excitations are contained in $\tilde{v}_{\mathbf{k}'\mathbf{k}}$. Thus, $\tilde{v}_{\mathbf{k}'\mathbf{k}}$ has a single-particle character as well as a many-particle character which arises from the Kondo resonance.

VI. LUTTINGER THEOREM

A. Numerical PRM result

Next let us study the Luttinger theorem, which relates the volume of the Fermi surface with the number of electrons [21]. Here, we start from a modified version of the Luttinger sum rule, which states that the conduction electron density is equal to the difference between the Fermi-surface volume and the volume of zeros in the Green's function [39,40]. Note that this version allows the Luttinger sum rule to survive in a Mott insulator, and we show in the following that it is also fulfilled for the Kondo lattice. The total number of particles n_c per site is given by:

$$n_c = \frac{1}{N}\sum_{\mathbf{k},\alpha}\langle c^{\dagger}_{\mathbf{k}\alpha}c_{\mathbf{k}\alpha}\rangle = \frac{S(S+1)}{2N^2}\sum_{\mathbf{k}}\sum_{\mathbf{k}'}|\tilde{v}_{\mathbf{k}'\mathbf{k}}|^2 f(\tilde{\varepsilon}_{\mathbf{k}'}), \quad (28)$$

where Eq. (23) was used. At $T = 0$, Eq. (28) reduces to

$$n_c = \frac{S(S+1)}{2N^2}\sum_{\mathbf{k}}\sum_{\mathbf{k}'}^{\tilde{\varepsilon}_{\mathbf{k}'}<0}|\tilde{v}_{\mathbf{k}'\mathbf{k}}|^2. \quad (29)$$

Only energies $\tilde{\varepsilon}_{\mathbf{k}'}$ below the Fermi-level ε_F contribute to Eq. (29). We emphasize again that the matrix elements $\tilde{v}_{\mathbf{k}'\mathbf{k}}$ contain contributions from both the one-particle excitations and the Kondo resonance. The latter represents the poles of the conduction electron self-energy in the Kondo lattice which usually arise due to the hybridization with the composite fermions. Here they appear as a result of the many-body effect between coherent excitations and localized spins. These contributions would lead to additional zeros in the conduction Green's function which instead are here straightforwardly counted within the momentum summation (29). This property allows us to evaluate the Luttinger sum rule without explicitly calculating Green's functions.

Relation (29) is again evaluated by solving the renormalization equations (18) and (19) for $v_{\mathbf{k}'\mathbf{k},\lambda}$ and $u_{\mathbf{k},\lambda}$. The result for n_c at $T = 0$ is shown in Table I for various values of the electronic-filling ν away from half-filling ($\nu = 1$). Obviously, the result shows that Luttinger's theorem,

$$n_c = \nu + 1 \quad (30)$$

is fulfilled. That is, the total number of particles per site at $T = 0$ is given by the filling ν of the pure free-electron system plus 1 where the number 1 corresponds to the concentration of the localized spins ($S = 1/2$). Thus, the PRM is able to verify Luttinger's theorem on the basis of a many-body approach. Relation (30) is one of the main results of the present work and adds to Oshikawa's topological proof of the Luttinger theorem for the Kondo lattice in Ref. [27]. The dependence of n_c on the filling ν is also demonstrated in Fig. 4 as follows: Changing the electron-filling ν, one finds that the complete structure around ε_F is merely shifted to lower or higher Fermi energies, depending on the lower or higher value of ν. Therefore, the Luttinger theorem (30) is automatically fulfilled if it is fulfilled for one filling.

TABLE I. Calculated total particle numbers for four different chosen values of the free conduction electron-filling ν. Within the numerical accuracy of the PRM approach the Luttinger theorem $n_c = \nu + 1$ is fulfilled for all the considered ν's.

Filling ν	Particle number n_c
0.22	1.2194
0.17	1.1691
0.13	1.1269
0.08	1.0748

B. Interpretation

Following the approximate expression (24) for $A(\mathbf{k}, \omega)$ one may also try to decompose n_c into two parts,

$$n_c = n_{c,\mathrm{el}} + n_{c,\mathrm{Kondo}}, \quad (31)$$

where the first contribution results from the renormalized single-particle excitations and the second one results from the Kondo excitations. With the help of Eqs. (28) and (23), we may express n_c as

$$n_c = \frac{2}{N}\sum_{\mathbf{k}}\int_{-\infty}^{\infty}A(\mathbf{k},\omega)f(\omega)d\omega, \quad (32)$$

where $f(\omega) = 1/(1 + e^{\beta\omega})$ is the Fermi function. Thus, with Eq. (21) we obtain in the $T = 0$ case,

$$n_c = \frac{S(S+1)}{2N^2}\sum_{\mathbf{k},\mathbf{k}'}|\tilde{v}_{\mathbf{k}'\mathbf{k}}|^2\int_{-\infty}^{0}\delta(\omega-\tilde{\varepsilon}_{\mathbf{k}'})d\omega, \quad (33)$$

where now the ω integral only allows negative frequencies. A decomposition of n_c according to Eq. (31) is found by introducing a $\mathbf{k}$-dependent boundary $\mathcal{C}_{\mathbf{k}}$ in the negative-ω space between the low-energy Kondo excitations and the high-energy dispersive excitations. This boundary is schematically shown in Fig. 1 (orange shaded area) for a selected $\mathbf{k}$ range in momentum space. In the actual calculations, we have defined $\mathcal{C}_{\mathbf{k}}$ by the ω position of the particular minimum of $A(\mathbf{k}, \omega)$ with respect to ω which is placed in the energy range between the dispersive excitation and the Kondo resonance. Using $1 = \Theta(\mathcal{C}_{\mathbf{k}} - \omega) + \Theta(\omega - \mathcal{C}_{\mathbf{k}})$, we find

$$n_c = \frac{S(S+1)}{2N^2}\sum_{\mathbf{k},\mathbf{k}'}|\tilde{v}_{\mathbf{k}'\mathbf{k}}|^2[\Theta(\mathcal{C}_{\mathbf{k}}-\tilde{\varepsilon}_{\mathbf{k}'})+\Theta(\tilde{\varepsilon}_{\mathbf{k}'}-\mathcal{C}_{\mathbf{k}})] \times\int_{-\infty}^{0}\delta(\omega-\tilde{\varepsilon}_{\mathbf{k}'})d\omega. \quad (34)$$

TABLE II. Calculated number of conduction electrons $n_{c,\mathrm{el}}$ and number of heavy quasiparticles $n_{c,\mathrm{Kondo}}$ for different chosen filling values ν. Our PRM approach confirms the prediction of the Luttinger theorem that the localized spins fully contribute to the Fermi volume as a system of occupied heavy quasiparticles, i.e., $n_{c,\mathrm{Kondo}} \approx 1$, whereas the "light" conduction electrons behave like free electrons, i.e., $n_{c,\mathrm{el}} \approx \nu$.

Filling ν	Electron number $n_{c,\mathrm{el}}$	Kondo excitations $n_{c,\mathrm{Kondo}}$
0.22	0.2247	0.9947
0.17	0.1731	0.9960
0.13	0.1314	0.9955
0.08	0.0812	0.9936

This leads to the decomposition (31) for n_c, where

$$n_{c,\mathrm{el}} = \frac{S(S+1)}{2N^2}\sum_{\mathbf{k},\mathbf{k}'}|\tilde{v}_{\mathbf{k}'\mathbf{k}}|^2\int_{-\infty}^{\mathcal{C}_{\mathbf{k}}(<0)}\delta(\omega-\tilde{\varepsilon}_{\mathbf{k}'})d\omega$$
$$= \frac{S(S+1)}{2N^2}\sum_{\mathbf{k}}\sum_{\mathbf{k}'}^{\tilde{\varepsilon}_{\mathbf{k}'}<\mathcal{C}_{\mathbf{k}}(<0)}|\tilde{v}_{\mathbf{k}'\mathbf{k}}|^2, \tag{35}$$

and

$$n_{c,\mathrm{Kondo}} = \sum_{\mathbf{k},\mathbf{k}'}|\tilde{v}_{\mathbf{k}'\mathbf{k}}|^2\int_{\mathcal{C}_{\mathbf{k}}(<0)}^{0}\delta(\omega-\tilde{\varepsilon}_{\mathbf{k}'})d\omega$$
$$= \frac{S(S+1)}{2N^2}\sum_{\mathbf{k}}\sum_{\mathbf{k}'}^{\mathcal{C}_{\mathbf{k}}<\tilde{\varepsilon}_{\mathbf{k}'}<0}|\tilde{v}_{\mathbf{k}'\mathbf{k}}|^2. \tag{36}$$

One easily realizes that decomposition (32) with Eqs. (35) and (36) corresponds to a generalization of decomposition (24) for $A(\mathbf{k},\omega)$. In expression (35) for $n_{c,\mathrm{el}}$ all excitations $\tilde{\varepsilon}_{\mathbf{k}'}$ are contained which have energies lower than the boundary $\mathcal{C}_{\mathbf{k}}$. Thus, if excitation $\tilde{\varepsilon}_{\mathbf{k}}$ belongs to the allowed values of $\tilde{\varepsilon}_{\mathbf{k}'}$, then Eq. (24) reduces to its coherent part. An equivalent argument is also true for $n_{c,\mathrm{Kondo}}$.

The numerical evaluation of both parts is given in Table II. Obviously, the results $n_{c,\mathrm{el}} \approx \nu$ and $n_{c,\mathrm{Kondo}} \approx 1$ are obtained, which are valid away from half-filling. Thus, the origin of the two parts contributing to Luttinger's theorem (35) has been identified.

In conclusion, in this paper we have applied a recently developed many-body technique to the Kondo-lattice model in $d = 2$. As one of the main results, we could verify Luttinger's theorem for this model. This paper presents a many-body study which is able to reproduce the correct value of this theorem. Note that our verification of Luttinger's theorem is only valid provided that the ground state of the Kondo lattice is a Fermi liquid. However, whether the model is a Fermi liquid is not trivial to answer. Instead, using *ansatz* (5) for $\mathcal{H}_{0,\lambda}$, we have assumed from the beginning that the Kondo lattice is a Fermi liquid.

ACKNOWLEDGMENTS

We thank J. van den Brink, H. Fehske, J. Geck, C. Hess, and J. Trinckauf for helpful discussions. We further thank U. Nitzsche for technical assistance. This project has received funding from the European Research Council (ERC) under the European Union's Horizon 2020 Research and Innovation Programme (Grant Agreement No. 647276–MARS–ERC-2014-CoG).

APPENDIX: DERIVATION OF THE RENORMALIZATION EQUATIONS FOR $u_{\mathbf{k},\lambda}$ AND $v_{\mathbf{k}'\mathbf{k},\lambda}$

The renormalization equations for the parameters of $\mathcal{H}_\lambda$ are derived from the transformation (3) together with the *ansatz* for $c^\dagger_{\mathbf{k},\lambda}$,

$$c^\dagger_{\mathbf{k},\lambda-\Delta\lambda} = e^{X_{\lambda,\Delta\lambda}}c^\dagger_{\mathbf{k},\lambda}e^{-X_{\lambda,\Delta\lambda}} = u_{\mathbf{k},\lambda}e^{X_{\lambda,\Delta\lambda}}c^\dagger_{\mathbf{k}}e^{-X_{\lambda,\Delta\lambda}}$$
$$+\frac{1}{\sqrt{N}}\sum_{\mathbf{k}'}v_{\mathbf{k}'\mathbf{k},\lambda}e^{X_{\lambda,\Delta\lambda}}\mathcal{D}^\dagger_{\mathbf{k}\sigma;\mathbf{k}'}e^{-X_{\lambda,\Delta\lambda}}. \tag{A1}$$

Expanding the exponentials for small $X_{\lambda,\Delta\lambda}$ (small Kondo exchange coupling j) one finds

$$c^\dagger_{\mathbf{k},\lambda-\Delta\lambda} = u_{\mathbf{k},\lambda}(c^\dagger_{\mathbf{k}} + [X_{\lambda,\Delta\lambda}, c^\dagger_{\mathbf{k}}] + \tfrac{1}{2}[X_{\lambda,\Delta\lambda},[X_{\lambda,\Delta\lambda},c^\dagger_{\mathbf{k}}]] + \cdots) + \frac{1}{\sqrt{N}}\sum_{\mathbf{k}'}v_{\mathbf{k}'\mathbf{k},\lambda}(\mathcal{D}^\dagger_{\mathbf{k}\sigma;\mathbf{k}'} + [X_{\lambda,\Delta\lambda},\mathcal{D}^\dagger_{\mathbf{k}\sigma;\mathbf{k}'}] + \cdots). \tag{A2}$$

Note that, for dominant order, $\mathcal{D}_{\mathbf{k}\sigma;\mathbf{q}}$ is of order j and $u_{\mathbf{k},\sigma}$ is of order j^0. Therefore, only the commutator $[X_{\lambda,\Delta\lambda},\mathcal{D}^\dagger_{\mathbf{k}\sigma;\mathbf{k}'}]$ is needed for the renormalization of $\mathcal{D}^\dagger_{\mathbf{k}\sigma;\mathbf{k}'}$, whereas for $c_{\mathbf{k}\sigma,\lambda}$ the commutators for first and second orders in j have to be taken into account.

Next, one is confronted with the evaluation of the commutators in Eq. (A2),

$$[X_{\lambda,\Delta\lambda}, c^\dagger_{\mathbf{k}\sigma}] = \frac{1}{\sqrt{N}}\sum_{\mathbf{k}'}X_{\mathbf{k}'\mathbf{k}}(\lambda,\Delta\lambda)\mathcal{D}^\dagger_{\mathbf{k}\sigma;\mathbf{k}'}, \tag{A3}$$

$$[X_{\lambda,\Delta\lambda},[X_{\lambda,\Delta\lambda},c^\dagger_{\mathbf{k}\sigma}]] = -\frac{1}{4N}\sum_{\mathbf{k}'}[X_{\mathbf{k}'\mathbf{k}}(\lambda,\Delta\lambda)]^2\langle\mathbf{S}_{\mathbf{k}'-\mathbf{k}}\cdot\mathbf{S}_{\mathbf{k}-\mathbf{k}'}\rangle c^\dagger_{\mathbf{k}\sigma} - \frac{1}{2\sqrt{N}}\sum_{\mathbf{q}}\Bigg[\frac{1}{N}\sum_{\mathbf{k}'}X_{\mathbf{k}'\mathbf{k}}(\lambda,\Delta\lambda)X_{\mathbf{k}'\mathbf{q}}(\lambda,\Delta\lambda)$$
$$\times(2\langle c^\dagger_{\mathbf{k}'\alpha}c_{\mathbf{k}'\alpha}\rangle - 1)\Bigg]\mathcal{D}_{\mathbf{k}\sigma;\mathbf{q}} + \frac{1}{2N^{3/2}}\sum_{\mathbf{q}\mathbf{k}'}X_{\mathbf{k}'\mathbf{k}}(\lambda,\Delta\lambda)X_{\mathbf{q}\mathbf{k}}(\lambda,\Delta\lambda)\langle\mathcal{K}_{\mathbf{k}'\mathbf{q}}\rangle c^\dagger_{\mathbf{k}\sigma}, \tag{A4}$$

and

$$[X_{\lambda,\Delta\lambda}, \mathcal{D}^{\dagger}_{\mathbf{k}\sigma;\mathbf{k}'}] = -\frac{1}{4\sqrt{N}} X_{\mathbf{k}'\mathbf{k}}(\lambda, \Delta\lambda) S(\mathbf{k}' - \mathbf{k}) c^{\dagger}_{\mathbf{k}\sigma} - \frac{1}{2N} \sum_{\mathbf{q}} X_{\mathbf{k}'\mathbf{q}}(\lambda, \Delta\lambda)(2\langle c^{\dagger}_{\mathbf{k}'\alpha} c_{\mathbf{k}'\alpha}\rangle - 1)\mathcal{D}^{\dagger}_{\mathbf{k}\sigma;\mathbf{q}}$$
$$+ \frac{1}{2N} \sum_{\mathbf{q}} X_{\mathbf{q}\mathbf{k}}(\lambda, \Delta\lambda)\langle \mathcal{K}_{\mathbf{k}'\mathbf{q}}\rangle c^{\dagger}_{\mathbf{k}\sigma}, \tag{A5}$$

where an additional factorization has been used. Inserting Eqs. (A3)–(A5) into (A2) and comparing with *ansatz* (13) (where λ is replaced by $\lambda - \Delta\lambda$) one is led to the renormalization equations (17) and (18).

[1] K. G. Wilson, Rev. Mod. Phys. **47**, 773 (1975).
[2] P. W. Anderson, *Valence Fluctuations in Solids* (North-Holland, Amsterdam, 1981).
[3] P. Coleman, Phys. Rev. B **28**, 5255 (1983).
[4] N. Read and D. Newns, J. Phys. C **16**, 3273 (1983).
[5] A. Auerbach and K. Levin, Phys. Rev. Lett. **57**, 877 (1986).
[6] C. Lacroix and M. Cyrot, Phys. Rev. B **20**, 1969 (1979).
[7] N. Read, D. M. Newns, and S. Doniach, Phys. Rev. B **30**, 3841 (1984).
[8] P. Coleman, Phys. Rev. B **29**, 3035 (1984).
[9] N. Read and D. M. Newns, J. Phys. C **16**, L1055 (1983).
[10] A. J. Millis and P. A. Lee, Phys. Rev. B **35**, 3394 (1987).
[11] P. Coleman, Phys. Rev. B **35**, 5072 (1987).
[12] P. Coleman, *Introduction to Many-Body Physics* (Cambridge University Press, Cambridge, UK, 2015).
[13] P. H. P. Reinders, M. Springford, P. T. Coleridge, R. Boulet, and D. Ravot, Phys. Rev. Lett. **57**, 1631 (1986).
[14] R. Settai, H. Shishido, S. Ikeda, Y. Murakawa, M. Nakashima, D. Aoki, Y. Haga, H. Harima, and Y. Onuki, J. Phys.: Condens. Matter **13**, L627 (2001).
[15] S. Paschen, T. Lühmann, S. Wirth, P. Gegenwart, O. Trovarelli, C. Geibel, F. Steglich, P. Coleman, and Q. Si, Nature (London) **432**, 881 (2004).
[16] R. Settai, H. Shishido, T. Kubo, S. Arakia, T. C. Kobayashi, H. Harimac, and Y. Onuki, J. Magn. Magn. Mater. **310**, 541 (2007).
[17] P. A. Lee, T. M. Rice, J. W. Serene, L. J. Sham, and J. W. Wilkins, Comments Condens. Matter Phys. **12**, 98 (1986).
[18] H. von Löhneysen, A. Shröder, M. Sieck, and T. Trappmann, Phys. Rev. Lett. **72**, 3262 (1994).
[19] A. H. C. Neto, G. Castilla, and B. A. Jones, Phys. Rev. Lett. **81**, 3531 (1998).
[20] J. M. Luttinger and J. C. Ward, Phys. Rev. **118**, 1417 (1960).
[21] J. M. Luttinger, Phys. Rev. **119**, 1153 (1960).
[22] R. M. Martin, Phys. Rev. Lett. **48**, 362 (1982).
[23] P. Coleman, I. Paul, and J. Rech, Phys. Rev. B **72**, 094430 (2005).
[24] H. Tsunetsugu, M. Sigrist, and K. Ueda, Rev. Mod. Phys. **69**, 809 (1997).
[25] K. Ueda, T. Nishino, and H. Tsunetsugu, Phys. Rev. B **50**, 612 (1994).
[26] R. Peters and N. Kawakami, Phys. Rev. B **92**, 075103 (2015).
[27] M. Oshikawa, Phys. Rev. Lett. **84**, 3370 (2000).
[28] J. Otsuki, H. Kusunose, and Y. Kuramoto, Phys. Rev. Lett. **102**, 017202 (2009).
[29] J. Otsuki, H. Kusunose, and Y. Kuramoto, J. Phys, Soc. Jpn. **78**, 034719 (2009).
[30] K. W. Becker, A. Hübsch, and T. Sommer, Phys. Rev. B **66**, 235115 (2002).
[31] S. D. Głazek and K. G. Wilson, Phys. Rev. D **48**, 5863 (1993).
[32] S. D. Głazek and K. G. Wilson, Phys. Rev. D **49**, 4214 (1994).
[33] S. Kehrein, *The Flow Equation Approach to Many-Particle Systems*, Springer Tracts in Modern Physics (Springer-Verlag, Berlin, 2006).
[34] F. Wegner, Ann. Phys. (Leipzig) **506**, 77 (1994).
[35] K. W. Becker, A. Hübsch, and S. Sykora (unpublished).
[36] S. Sykora and K. W. Becker, Sci. Rep. **3**, 2691 (2013).
[37] S. Cottenier, S. N. Mishra, S. Demuynck, J. C. Spirlet, J. Meersschaut, and M. Rots, Phys. Rev. B **63**, 195103 (2001).
[38] M. Siahatgar, B. Schmidt, G. Zwicknagl, and P. Thalmeier, New J. Phys. **14**, 103005 (2012).
[39] A. A. Abrikosov, L. P. Gorkov, and I. E. Dzyaloshinski, *Methods of Quantum Field Theory in Statistical Physics* (Dover, Mineola, NY, 1975).
[40] A. M. Tsvelik, *Quantum Field Theory in Condensed Matter Physics* (Cambridge University Press, Cambridge, UK, 2007).